Establishment of 3D Spheroid Human Dermal Papilla Cells as an Effective Model for Hair Growth Screening Compounds Compared with the 2D System: An Example of Minoxidil and 3,4,5-Tri-O-caffeoylquinic acid (TCQA)

Meriem Bejaoui
AIST-University of Tsukuba
Aprill Kee Oliva
Arena
May Sin Ke
University of Tsukuba: Tsukuba Daigaku
Farhana Ferdousi
University of Tsukuba: Tsukuba Daigaku
Hiroko Isoda (isoda.hiroko.ga@u.tsukuba.ac.jp)
University of Tsukuba: Tsukuba Daigaku https://orcid.org/0000-0002-1399-9541

Research

Keywords: 3D spheroid cell culture, Human follicular dermal papilla, Minoxidil, TCQA, ECM

Posted Date: November 23rd, 2021

DOI: https://doi.org/10.21203/rs.3.rs-1038276/v1

Abstract

Introduction

Dermal papilla cells (DPc) is an important element in studying the hair follicle (HF) niche. The human hair follicle dermal papilla cells (HFDPC) are widely used as an in vitro model to study hair growth related research. These cells are usually grown in 2D culture, nevertheless, this system did not show efficient therapeutic effect on HF regeneration and growth, and key differences were observed between cell activity in vitro and in vivo.

Objective

Recent studies have showed that HFDPC grown in 3D hanging spheroids is more morphologically akin to intact DPc microenvironment. This current study showed that the 3D model is applicable to the commercial cell line with new insights on its variability by comparing to previous studies of gene signature restored by 3D culture.

Methods and Results

Our data demonstrated that HFDPCS grown in 3D in vitro model can influence not only hair growth-related pathways but also immune system -related pathways compared to 2D cell monolayer. Furthermore, we compared the expression of signalling molecules and metabolism-associated proteins of HFDPC in minoxidil (FDA approved drug for hair loss treatment) and 3,4,5-tri-O-caffeoylquinic acid (TCQA) (recently found to induce hair growth in vitro and in vivo) treated 3D and 2D cell cultures using microarray analysis.

Conclusion

Further validation of the results confirms the suitability of this cell line for 3D model while providing new insights such as to the mechanisms behind the hair growth effects of 3D spheroid treated with hair growth promoting agents.

Introduction

It has been known for a long time that the hair follicle (HF) undergoes continuous cycling that is categorized into three stages, expansion (anagen), apoptosis-driven regression (catagen), and inactivity (telogen) [1]. The HF contains different cell population distinct in their function, molecular mechanism, and origin that throughout adult life are revived from niche-resided stem cells located in the bulge [2].The growth cycle and cells regeneration is mainly controlled by a group of specialised fibroblastic cells of mesenchymal origin, known as the dermal papilla cells (DPc) [3].

The longest stage within the hair cycle in human, is the anagen stage which takes 2 to 5 years. As for the second phase, it occurs from few days to few weeks, while the telogen usually takes 3 months, for the

normal hair cycle [1]. However, some disturbances can interfere in the process causing premature termination of the anagen and an early onset of the catagen and telogen phases [4]. These dysregulations may lead to the miniaturization of hair shaft (HS) and/or a higher number of hairs in the catagen-telogen phase which will results to hair loss and eventually alopecia [5–7]. These irregularities can appear in DPc, thus discovering new insights regarding how to battle hair loss using cultured DPc is still a focus point for a lot of researches. The human hair follicle dermal papilla cells (HFDPC) are mainly used in two-dimensional (2D) culture and this system have been the more broadly studied as a form of hair growth *in vitro* model for its simplicity and efficient culturing workflows [8]. However, 2D cultured DPc have demonstrated no therapeutic effect on HF growth and this raised questions as to the suitability of this model to study hair growth cycle and hair regeneration [9].This is explained by the necessity of communication between the epidermal cells and DPc to regulate the hair growth cycle and for this reason the cells primarily exist in topographically complex and three-dimensional (3D) extracellular environments within the HF [10]. Attached to a collagen-coated polystyrene surface, the 2D configuration deeply constrains the usual cell environment that can highly cause the remodelling of DPc behaviour [11,12]. Thus, 2D monolayer cell culture do not reflect the actual 3D environment where the communication occurs between cell-cell , and cell- extra cellular matrix (ECM) within a specific cellular organization required for hair growth and regeneration [13].

Recently, an expansion of evidence and documentation has indicated that 3D cell culture systems represent more accurately the microenvironment surrounding the tissue [14]. In this system, the cells present morphological and physiological difference reflecting *in vivo* cellular responses, comparing to 2D cultured cells [15,16]. Interestingly, 3D culture system is gaining insight not only because it affects the dimensional organization of the cell allowing the communication with neighbouring cells, but also it influences the signal transduction, gene expression, and cellular behaviour [17,18]. Based on previous studies, 3D DPc cultured in spheroid system using the hanging drop technique, may restore partially hair inductivity potential of intact DPc lost in 2D culture as it encourages the formation of condensate-like structure [9,19]. However, spheroid cell culture systems may present limitations that are a rather not strong interaction with the extracellular environment, and, an inconsistency in the expression of selected 3D markers and hair inductive potential of 3D DPc cultures was found [8,9].

Alopecia is an exceedingly prevalent hair loss condition affecting many people worldwide and hence attracts demands for treatment [20]. Only two drugs have approved by the Food and Drug Administration (FDA) as a treatment of hair loss, one of which is minoxidil. Our group have previously published that the polyphenolic compound, 3,4,5-tri-*O*-caffeoylquinic acid (TCQA) significantly activated Wnt/β-catenin signalling *in vivo* and in HFDPC for the promotion of hair growth cycle and pigmentation [21,22]. Next, TCQA was found to promote the differentiation of 3D cultured human amnion epithelial stem cells while increasing ECM markers [23]. Consequently, high demand for using target compounds known to promote hair growth and ECM related markers to overcome the limitations of 3D spheroid DPc culture.

Hence in this paper, we compared the expression of signalling molecules and markers of HFDPC commercial cell line in untreated 3D and 2D cell cultures using microarray analysis. By evaluating the

gene signature of 3D culture in comparison to 2D, we investigate whether this commercial cell line is able to successfully express the gene signatures of a 3D spheroid and represent a closer to intact DP hair growth metabolism. Our data demonstrated that the commercial cell line grown in 3D *in vitro* model can influence not only hair growth related pathways but also immune system related pathways compared to 2D cell monolayer. This study aim to establish HFDPC 3D model as the adequate system to represent DP microenvironment. Moreover, we report the molecular mechanism behind minoxidil and TCQA hair growth promotion effect in 3D and 2D culture model, used to further establish this technique as a validate model for hair related research.

Materials And Methods

Samples Preparation

Minoxidil was bought from Tokyo Chemical Industry (Tokyo, Japan).TCQA was synthesized with 97% purity. The two sample were prepared in 70% ethanol prior to dilution in the growth medium for *in v*itro assay.

Cells and cell culture

HFDPC were purchased from Cell Application Inc. (Tokyo, Japan). The cells were kept in appropriate medium (Toyobo, Osaka, Japan) supplemented with growth factors (Toyobo, Osaka, Japan).

For the 2D model, HFDPCs were cultured in dermal papilla growth medium. Prior to seeding or passage, the plate were coated with collagen solution (Toyobo, Osaka, Japan) for 2 h at room temperature (RT). The cells were monitored under sterile conditions at 37 °C in a humidified atmosphere of 5% CO_2.

Establishment and maintenance of 3D culture.

HFDPC were cultured in 3D spheroids system [9]. Firstly, cells were cultured without antibiotics in papilla cell growth medium. The seeded cells were trypsinized, 5 ml of the culture medium was added, the cells were centrifuged, and then resuspended at 300 cells per µl, 48 h post passage. The 3D culture was established using hanging drops methods on the lid of a 100-mm petri dish. Each 10 µl hanging drop contains approximately 3,000 cells, phosphate-buffered saline (PBS) was placed to completely cover the base of the dishes. Two group were established, the control group (untreated cells) were the drop were formed from the culture medium containing the cells, and the treated groups with 0.1 and 10 µM, minoxidil and TCQA, respectively. The formation of spheroid using hanging drops method was established after 48 h, 3D spheroid DPc were then used in the following experiments.

RNA extraction

The RNA was extracted from HFDPC cultured in 3D and 2D systems. For the 2D system, HFDPC were seeded overnight (5×10^5 cells per 100-mm dish), then the papilla medium was renewed with the treatment (0, 0.1 µM minoxidil, and 10 µM TCQA). After 48 h, the medium was discarded, a washing with

cold PBS was assessed following by an Isogen extraction (Nippon Gene, Tokyo, Japan) according to the manufacturer's directions. Also 3D hanging drops untreated and treated with 0.1 μM minoxidil, were subjected to the same procedure. For both systems, the RNA concentration was assessed using a NanoDrop 2000 spectrophotometer.

DNA microarray analysis

The extracted RNA samples extracted from 2D and 3D system were prepared for microarray analysis using GeneChip® 3' Expression Arrays and 3' IVT PLUS Reagent Kit (Affymetrix Inc, CA, United States). In brief, (250 ng) was used to generate amplified and biotinylated aRNA following the manufacturer protocol. The array strips (HG-U219) were hybridized for 16 h in a 45°C station, then washed, stained, and imaged in the GeneAtlas Fluidics and Imaging Station.

For the analysis, firstly the Expression Console Software was used for the raw data normalization, allowing the selection of genes with a fold change > 1.4 (in linear space) and P-value ≤0.05 (One-way between-subject ANOVA) to be designed as differentially expressed genes (DEGs). Further analysis was carried out using Transcriptome Analysis Console (TAC) version 4, Database for Annotation, Visualization, and Integrated Discovery (DAVID), Gene Set Enrichment Analysis (GSEA), ExAtlas: gene expression, and Meta-analysis [24–26].

Quantitative real-time PCR analysis

The RT-PCR analysis was performed using SuperScript IV reverse transcription kit (Invitrogen, CA, USA). TaqMan Universal PCR mix and TaqMan probes specific), *CTNNB1* (Hs99999168_m1), *ALPL* (Hs01029144) *NCAM* (Hs00941830_m1), and VCAN (Hs00171642_m1) (Applied Biosystems, CA, USA) were used in the 7500 Fast Real-Time PCR Software 1.3.1. GAPDH (Hs 02786624_ g1) (Applied Biosystems, CA, USA) was used as endogenous control.

Western blot

The protein were extracted from HFDPCs cultured in 2D and system and treated with or without 0.1 μM minoxidil after 48 h as explained above. Total protein extraction was achieved using radio-immunoprecipitation assay (RIPA) buffer (SIGMA, Saint Louis, USA) and protease inhibitor, and quantified with the 2-D Quant kit (GE Healthcare, Chicago, USA).

The proteins were separated in the SDS-PAGE, and the transfer was carried out in a PVDF membrane (Millipore, NJ, USA). After blocking, the membranes were incubated with primary antibodies against VCAN (Abcam, Rockford, USA), NCAM (Abcam, Rockford, USA), β-catenin 71-2700 (Thermo Fisher Scientific, Massachusetts, USA), ALP (Abcam, Rockford, USA), FGF1 (Abcam, Rockford, USA), and GAPDH sc32233 (Santa Cruz 1 Biotechnology, Texas, USA). After overnight incubation at 4°C, the second antibody goat anti-rabbit IRDye 800 CW or IRDye 680 LT goat anti-mouse were added. Then the signal was detected using LI-COR Odyssey Infrared Imaging System (LI-COR, NE, USA).

Statistical analysis

Results were expressed as mean ± standard deviation (SD). Statistical analysis was performed using Student's t-test when comparing two value sets For microarray analysis, ANOVA (One-way between-subject ANOVA unpaired) was performed to assess the level of significance between treated groups.

Results

Gene profiling analysis of HFDPCs cultured in 3D hanging compared with 2D culture

To determine whether there is successful spheroid formation, we compared the consistency of spheroid size and shape formation using gene expression analysis. To understand the integrative response of 3D culture, we assigned the cut off for the differentially expressed genes (DEGs) to be >2.0 or <2.0 (linear fold change). We found 1933 genes between 2D and 3D samples to be consistently differentially expressed. Of these genes, 823 genes were upregulated and 1110 genes were downregulated as s represented in the volcano plots that show the distribution of fold change and significance levels of the DEGs (**Figure 1A**).

Gene set enrichment analysis of 3D control compared with 2D control showed the upregulation of several prior defined hallmark gene sets associated with collagen regulation (GO:0005587, GO:0005518, GO:0062023), cell adhesion (GO:0007155), endothelial cell proliferation (GO: 0001938), and cellular response to UV (GO:0034644) (**Figure 1B**). Interestingly, immune system significant gene were regulated in 3D system compared with 2D (**Figure 1C**).

The results were further validated to show the formation of the 3D structure and the cell adhesion of HFDPCs. The expression of Versican (VCAN) and Neural cell adhesion molecule (NCAM) involved in cell adhesion were checked. Figure 1D and E displayed the upregulation of the expression of these molecules on the gene and protein level in HFDPCs cultured in 3D compared with 2D after 48 h.

Moreover the highly regulated genes in 3D spheroid were classified in Table 1 to summarize the finding data. These results showed that 3D system further enhance the cell-cell and cell- ECM interactions, and confer a better defence response and a more resistant immune system.

Comparison of the DEGs in 3D and 2D cultured HFDPCs treated with Minoxidil

The cells were cultured in 3D and 2D system and treated with 0 and 0.1 μM for 48 h, then microarray analysis was performed and the DEGs were to be >1.3 or <-1.3 (linear fold change). Results revealed the regulation of 594 out of which 225 are upregulated while 369 downregulated in case of 2D minoxidil vs 2D control (**Supp Figure 2A**). In case of 3D minoxidil vs 3D control, 5160 are upregulated and 6316 are downregulated (**Supp Figure 2B**). Then the DEGs were classified into different categories according to fold-change. For the 3D system, more genes with 2-fold change and-2-fold change were upregulated and downregulated, respectively (**Supp Figure 2C**). The top 100 DEGs in the treated groups: 3D minoxidil, 3D control, 2D minoxidil, and 2D control, were subjected to hierarchical clustering. Results demonstrated that

the top genes displays different expression between 3D minoxidil vs 3D control and 2D minoxidil vs 2D control (**Supp Figure 2D**).

3D cultured HFDPCs treated with Minoxidil upregulated hair growth-associated pathways

First of all to know minoxidil mechanism of action, we analysed the gene profiling of 2D minoxidil vs 2D control and 3D minoxidil vs 2D control. Results revealed that 2D minoxidil affected *CTNNB1,* Wntless *(WLS),* fibroblast growth factor 7 (*FGF7),* bone morphogenetic protein 1 *(BMP1)*, and collagen 5A (*COL5A)*, these genes are linked with Wnt/β-catenin, FGF, BMP, and collagen pathways (**Supp Table 1**). A downregulation of genes linked with collagen breakdown including matrix metalloproteinase molecules: *MMP24, MMP7,* and *MMP8*, and Wnt/β-catenin repression such us *TAXIBP3*, was observed (**Supp Table 2**). Minoxidil treatment in 2D-cultred HFDPCs enhanced hair growth-associated genes mainly Wnt/ β-catenin pathway. In addition, minoxidil treatment in 3D-cultred HFDCPs upregulated *CTNNB1* as well, *ABCC11* (ATP binding), collagen adhesion, and cell adhesion molecule like: *NCAM* and *VCAN* (**Table 2**). On the other hand the expression of genes significant for telogen phase, stem cells quiescence was significantly decreased upon minoxidil treatment in 3D-cultred HFDPCs (**Table 3**).

Heat map was created to compare 3D minoxidil with 2D minoxidil. We observed the enhancement of the expression of genes significant for cell-cell adhesion (GO: 0098609), Wnt signalling (GO: 0060071), positive regulation of canonical Wnt signalling (GO: 0090263) tricarboxylic acid cycle (GO: 0006099), cell cycle arrest (GO: 0007050) (**Figure 2A**). On the other hand, 3D minoxidil treatment inhibited genes linked with interferon production (GO: 0032728), NF-kappaB signalling (GO: 0043123), and apoptotic signalling (GO: 1900740) (**Figure 2A**). The molecular function and the Kegg pathway analysis of the DEG showed that 3D minoxidil treated upregulated ATP binding pathways, cell cycle, and fatty acid metabolism compared with 2D minoxidil treatment (**Figure 2B**).These current data demonstrated that minoxidil stimulated hair growth associated genes, ATP and collagen binding but the effect was higher in 3D cultured cells.

Moreover, to prove that the upregulation of hair growth-, cell adhesion-, and collagen binding-associated genes was due to minoxidil treatment not only to the 3D structure, a comparison of the DEGs between 3D control vs 2D control and 3D minoxidil vs 2D minoxidil was assessed. Supp Fig 2A illustrated the obtained data, and the common upregulated genes between these two set are only 12, whereas the 3D minoxidil upregulated genes more linked with cell cycle arrest, inflammation response compared with the 2D minoxidil. For the downregulated genes between the previously stated set, the common genes are 11 and 3D minoxidil significantly decreased the expression of genes linked with inflammation and cell division (**Supp Fig 2B**).

These results showed minoxidil treatment to 3D cultured HFDPCs highly affected hair growth associated pathway and markers, and cell cycle arrest signalling while conferring an anti-inflammatory activity.

*3D cultured HFDPCs treated with Minoxidil enhanced the gene and protein expression of hair growth marker***s**

Firstly, the gene expression of *NCAM* and *VCAN* was assessed upon minoxidil treatment in 3D cultured HFDPCs, because of their function as adhesion molecule essential to validate the formation of 3D spheroid, and also the implication in keratinocytes differentiation. Results revealed that minoxidil enhanced the expression of these markers confirming that the treatment did not affect the establishment of the 3D structure (**Figure 3A**).

The highly affected pathway by minoxidil treatment weather in 2D or 3D culture system are the Wnt/β-catenin and FGF pathways, and dermal papilla marker alkaline phosphatase or ALP. The gene and protein expressions of these markers were checked and results showed the upregulation upon treatment. We take the example of β-catenin, where minoxidil treatment enhanced the gene expression up to 1.8- and 2.8-fold change, and the protein expression up to 1.4- and 2.2-fold change, respectively, in the case of 2D and 3D structure (**Figure 3B and C**). We observed the same tendency in case of FGF-related molecules and ALP. These data demonstrated that minoxidil treatment in the 3D system had a higher effect in the regulation of hair growth in dermal papilla cells comparing with the 2D model.

Characteristics of 2D and 3D cultured HFDPC treated with TCQA

In this study we used another compound to test the efficacy of 3D system, TCQA was previously reported to stimulate the anagen phase and the hair growth cycle in C3H mice and in HFDPCs [22]. After 48 h, 2D cultured HFDPCs grew in the conventional monolayer format, in contrary, the 3D cultured HFDPC exhibited intercellular aggregation (**Figure 4A**).

To elucidate the characteristics of the cells cultured in 2D and 3D and simultaneously treated with TCQA, gene profiling analysis was assessed. The result showed that genes sets namely Wnt signalling pathway, epithelial-mesenchymal cell differentiation, collagen, cell-cell adhesion, fibroblast proliferation, were significantly upregulated upon TCQA treatment (**Figure 4B and C**). This is to further determine the extent of gene expression difference between the two used cell culture methods, important top upregulated and downregulated genes were picked and classified in Tables. Wnt signalling and anagen induction genes were modulated specifically *CTNNB1, Wnt11, WLS*, and *ALPL*, along with *FGF1* and *FGF5* (**Supp Table 3, 4 and 5**). Others factors involved in HF regeneration and hair cycle regulation such us *SOX4, NRAS, BMPR-1A* and *BMP5* was as well enhanced upon treatment. It is worth to mention that VCAN a marker of 3D spheroid formation and fibroblast differentiation was upregulated in 2D and 3D system. While this is true for both 2D and 3D culture, the genes in the TCQA-treated 3D culture exhibited a more than double fold-change in comparison to the fold change in the 2D monolayer cultured cells (**Supp Table 3 and 4**). *CTNNB1* expression was stimulated up to 1.62-fold change in TCQA-treated 2D HFDPCs, while in TCQA-treated 3D HFDPCs, the expression was up to 43.57-fold change. These results showed that the effect of TCQA on stimulating hair growth-related genes was more pronounced and significantly higher in the 3D spheroid system compared with the 2D.

Furthermore, genes involved in protein binding, PI3K-AKT signalling pathway, DNA damage, alternative splicing, phosphoprotein and negative regulators of cell functions were downregulated (**Figure 4D and E**). Supp Table 3 and 5 illustrated the repression of genes linked with Wnt/ β-catenin inhibition, telogen

phase regulation, anagen phase delay, and collagen breakdown for both 2D and 3D cultures (*TCF3, LDB3, AXIN2, GSK3B,* and *EGR1*). We noticed as well the pattern, that the fold-change was further decreased in case of 3D cultured compared with the 2D upon TCQA treatment. In addition, the DEGs between 3D TCQA vs 3D control with 2D TCQA vs 2D control were compared and Veen diagram was created for both upregulated and downregulated genes (**Figure 4F and G**). Results revealed that few genes were common between the two compared sets and the top DEGs were summarized in Supp Table 3 to 5.

The results of microarray in this study were compared to the *in vivo* microarray result from the back skin of eight-weeks-old C3H male mice treated topically for one month with TCQA upon shaving [22]. Table 5 displays the fold-change comparison of 2D-, 3D TCQA-treated HFDPCs, and *in vivo* microarray result. It showed that 3D cultured TCQA-treated HFDPC exhibited an extraordinarily high level of fold change compared to 2D and *in vivo* data mainly linked to canonical Wnt signalling (**Table 4**).

Some of the DEGs were validated by Quantitative RT-PCR. Result showed that the gene expression of 3D culture structure markers: *NCAM* and *VCAN* were enhanced upon TCQA treatment (**Figure 5A**). This suggests that TCQA's ability to express these genes higher in 3D, is vividly due to better cell-cell interaction in between the dermal spheroids. *CTNNB1*, *ALPL*, and *FGF1* gene expression is significantly expressed by TCQA both in 2D- and 3D-treated HFDPCs, however, comparison showed that 3D-HFDPC-treated with TCQA expressed the said gene significantly higher than 2D (**Figure 5B**). Thus, these data revealed that TCQA enhanced hair growth-related pathways, decreased telogen- and Wnt repression-significant genes, and this effect is more evident in 3D culture systems.

Discussion

The HF neogenesis is considered as an attractive target for regenerative medicine purposes, in part due to, the strong foundation of knowledge underpinning the HF biology, and widespread clinical interest [9]. One of the approaches to induce the anagen phase of hair growth cycle is the replenishment of DPs cells with *in vitro* 2D-cultured DPc, yet, with this technique the cells will lose their hair-inducing capacity over time because they are cultured on a flat, plastic surface [27]. Numerous studies have showed that 2D-cultred DPc were unable to induce anagen-telogen transition upon in situ implantation after 6 passages, as these cells needs to agglomerate in the HF to be highly active [28–30]. To overcome this problem, 3D spheroid culture is considered to be an efficient tool to regain DPc inductive capacity which may enable them to induce de novo HF in human skin as these cells requires cross-talk with the surrounding environment [5,31]. Nevertheless, an extensive knowledge of the molecular mechanisms governing the regenerative process is necessary. In this study, global gene profiling analysis was performed to compare 3D spheroid with 2D-cultured HFDPCs to determine the signature regulating the inductive phenotype of DPc. In addition, we compared the effect of alopecia approved drug minoxidil, and the polyphenolic compound TCQA recently published and found to enhance hair growth *in vivo* and *in vitro*, in 3D and 2D culture systems.

Generally, cell growth within a spheroid structure, facilitate DPc cell aggregation and cohesion which the loss of these two functions may bring, papilla miniaturization, disturbance of adult HF morphogenesis, and eventually hair loss [32,33]. Our data confirmed as well what was previously discussed that in case of 3D spheroid DPc, the GO of collagen regulation, cell adhesion, ECM, and cell proliferation were positively stimulated (**Figure 1**). The ECM plays a major role for the cell growth and adhesion, and cell-cell interaction. A common physiological feature of DPc is their close contact with the ECM, which is proved to be further enhanced in 3D spheroid culture [34,35]. For *in vitro* studies involving DPc, NCAM and VCAN has been used as major indicators for the inductive capabilities of these cells, accordingly the decrease in their expression correlates with the decline of DPc inductive capacities [36,37]. NCAM is involved in dermal condensation and hair induction, whereas VCAN is not only implicated in matrix assembly and structure and in cell adhesion, but also in HF development and cycling [38–40]. Our study has showed that in 3D spheroids, the expression of these DPc markers was higher compared with 2D culture system (**Figure 1**).

Putting all together, restoring human DPc inductivity via the artificial recreation of the cells 3D architecture and intercellular contacts using 3D spheroid cultures, considered to be an efficient method [41]. Nevertheless, while this technique allowed a partial restoration of DPc native signature and transcriptome, it have showed a limitation in human-human recombinant assay as the 3D spheroid could only stimulate the hair induction by 15% [9]. Thus, the need to address new strategies in order to properly recover the inductive capacities of DPc. For this purpose, using compounds and biomolecules able to activate hair growth related pathways in 3D spheroids system, can be considered as a capable approach to further enhance DPc inductive properties [42,43]. Therefore, in this current research, minoxidil the FDA approved drug against alopecia and TCQA a polyphenolic compound reported to stimulate hair growth were tested in 3D spheroids systems. Minoxidil affects hair growth cycle whether in animal models or human clinical trials by, shortening the length of the telogen phase, increasing the rate of DNA synthesis in anagen bulbs causing an early entry to the anagen phase [44–46]. An experimental study with 2D cultured DPc have reported that minoxidil prolonged the anagen phase by inducing prostaglandin E2 and β-catenin activity, and stimulating follicular proliferation and differentiation [47,48]. To the best of our knowledge, minoxidil mechanism of action in 3D spheroid DPc is not yet explored. Here, we reported that minoxidil upregulated of hair growth-, cell adhesion-, ATP binding- and collagen-associated in 3D system compared with 2D (**Figure 2**). The proliferation of DPc during the anagen phase is usually followed by an increase in the ATP content resulting in the expansion of cell size which will directly affect the differentiation of keratinocytes into the HS [49,50]. The extracellular matrix category included several collagens in addition to other transcripts that are expressed in the intact DP [51], which were found to be more present in 3D minoxidil-treated spheroid compared with the 2D (**Figure 2**, **Table 2**). Next, 3D minoxidil downregulated genes repressing Wnt/β-catenin pathway (*AXIN2*) and telogen marker *NFATC1* (**Table 3**). Axin2 is involved in β-catenin phosphorylation, degradation and non-translocation to the nucleus, leading to a shorten anagen phase in the HF. Nfatc1 plays a role in HF stem cells quiescence which is explain it high expression during the telogen phase , and the decreases during the transition to anagen favoring stem cells differentiation [52–54]. Moreover, gene expression analysis data was

supported by the increase of the gene expression of *NCAM* and *VCAN*, and the gene and the related proteins expression of hair growth makers: *ALPL* (ALP), *FGF1* (FGF1), and β-catenin (*CTNNB1*) in the 3D spheroid compared with the 2D (**Figure 3**). As mentioned earlier in this paper, several molecular markers have been used as an indicator of hair inductiveness, including VCAN and NCAM. Additionally, numerous studies have discussed that increasing VCAN expression in DPc enable HF induction and stimulate growth cycle initiation, suggesting its expression correlates with hair inductivity [55,56]. ALP is a known marker of DPc, overexpressed during the growth phase of the hair cycle while FGF1 is required in the promotion of the growth phase in C57BL/6 mice [7,57,58]. The role of β-catenin is well documented and established in the regulation of hair growth, as it is highly expressed during anagen phase in the DPc, and the absence of which induces a premature catagen phase [5,59,60]. Putting all together, the expression of hair growth markers was more pronounced in 3D model compared with 2D one, and minoxidil treatment further enhanced the efficacy of the 3D spheroid system in DPc.

On the other hand, TCQA was previously reported to have the ability to promote hair growth in CH3 mice and in HFDPCs via the activation of β-catenin [22] .Therefore, TCQA's capability to activate Wnt/beta-catenin signalling to induce hair growth in 3D spheroid DPc was investigated. TCQA-treated 3D culture exhibited a higher expression of gene sets related to Wnt/beta-catenin pathway, cell proliferation and collagen compared to the 2D culture (**Figure 4 and 5**). Canonical Wnt pathway serves as the central regulator of hair morphogenesis and cycling, and different type of Wnt have various roles in the HF regeneration [61]. Additionally, 3D-TCQA-treated cells highly expressed some collagen-related genes like COL3A1 (**Supp Table 4**). This a type III collagen, also known as fibrillar collagen found in skin mainly associated with the papillary dermis, produced by intact DPc, and responsible for HF development [62]. The comparison of the genes between, TCQA treated-DPc in 2D and 3D system, with TCQA treated mice skin previously published [22], listed on Table 4 clearly showed that the fold change of the selected genes greatly differs. Fold change in the TCQA-treated 3C culture is more than double for some genes compared to the 2D monolayer culture, and surprisingly, it showed that the fold change for the 3D system is higher than *in vivo* model. Taken altogether, despite TCQA's positive effect on 2D cultured-DPc, the full potential of the compound when studied in culture was highly compromised. Cellular aggregation mimics the microenvironment of dermal papilla, thus restoring the cues that happened on its normal niche. Therefore, the effect of this compounds was higher in 3D spheroid DPc compared with 2D system.

Overall, we have demonstrated that the partial reprogramming of HFDPC by spheroid formation with the addition of hair growth stimulating compounds can restore further restore the inductive capacities of DPc. These findings represent a significant leap for both, 3D spheroid DPc culture method and for minoxidil and TCQA as hair promoting agents.

Abbreviations

HFDPCs: Human Hair Follicle Dermal Papilla Cells

TCQA: 3,4,5-Tri-*O*-Caffeoylquinic Acid

HF: Hair Follicle

DPc: Dermal Papilla Cells

HS: Hair Shaft

2D: Two-Dimensional

3D: Three-Dimensional

ECM: Extra Cellular Matrix

FDA: Food and Drug Administration

RT: Room Temperature

PBS: Phosphate Buffered Saline

RMA: Robust Multichip Average

TAC: Transcriptome Analysis Console

DEGs: Differentially Expressed Genes

DAVID: Database of Annotation, Visualization, and Integrated Discovery

GSEA: Gene Set Enrichment Analysis

RIPA: Radio Immunoprecipitation Assay

SD: Standard Deviation

GO: Gene Ontology

FGF: Fibroblast Growth Factor

BMP: Bone Morphogenetic Protein

ALP: Alkaline Phosphatase

Declarations

Ethics Approval and Consent for Publication

Full consent for the publication of the performed experiments was obtained

Acknowledgements

We would like to thank Dr. Kozo Sato from Synthetic Organic Chemistry Laboratories, the FUJIFILM Corporation (Kanagawa, Japan) for providing synthesized TCQA.

Data availability

The data that support the findings of this study are available within the paper. The microarray data have been deposited to NCBI, GEO database (accession: GSE178510 and GSE178637

https://www.ncbi.nlm.nih.gov/geo/query/acc.cgi?acc=GSE178510

https://www.ncbi.nlm.nih.gov/geo/query/acc.cgi?acc=GSE178637)

Competing Interests

The authors declare that they have no financial or commercial conflicts of interest.

Author's contribution

MB and AKO performed most of the experiment data analysis and interpretation, prepared the figures, and wrote the manuscript. MKS prepared the sample, participated it in the data curation and validation, edited and revised the manuscript. FF was involved in the microarray analysis, edited and revised the manuscript. HI conceived and supervised the study, managed funding and resources for the study and reviewed the manuscript. All authors read and approved the final manuscript

Funding

This study was supported by Japan Science and Technology Agency (JST); Science and Technology Research Partnership for Sustainable Development (SATREPS, Grant No. JPMJSA1506).

References

[1] M.R. Schneider, R. Schmidt-Ullrich, R. Paus, The Hair Follicle as a Dynamic Miniorgan, Curr. Biol. 19 (2009) R132–R142. https://doi.org/10.1016/j.cub.2008.12.005.

[2] K.S. Stenn, R. Paus, Controls of hair follicle cycling, Physiol. Rev. 81 (2001) 449–494. https://doi.org/10.1152/physrev.2001.81.1.449.

[3] R. Paus, G. Cotsarelis, T He B Iology of H Air F Ollicles, New Engl. Jouranal Med. 341 (1999) 491–497.

[4] S. Malkud, Telogen Effluvium: A Review, J. Clin. Diagn. Res. 9 (2015) WE01-WE3. https://doi.org/10.7860/JCDR/2015/15219.6492.

[5] D. Enshell-Seijffers, C. Lindon, M. Kashiwagi, B.A. Morgan, β-catenin Activity in the Dermal Papilla Regulates Morphogenesis and Regeneration of Hair, Dev. Cell. 18 (2010) 633–642.

https://doi.org/10.1016/j.devcel.2010.01.016.

[6] V.-L. Truong, M.J. Bak, C. Lee, M. Jun, W.-S. Jeong, Hair Regenerative Mechanisms of Red Ginseng Oil and Its Major Components in the Testosterone-Induced Delay of Anagen Entry in C57BL/6 Mice., Molecules. 22 (2017). https://doi.org/10.3390/molecules22091505.

[7] R.R. Driskell, C. Clavel, M. Rendl, F.M. Watt, Hair follicle dermal papilla cells at a glance, J. Cell Sci. 124 (2011) 1179–1182. https://doi.org/10.1242/jcs.082446.

[8] N. Betriu, C. Jarrosson-Moral, C.E. Semino, Culture and Differentiation of Human Hair Follicle Dermal Papilla Cells in a Soft 3D Self-Assembling Peptide Scaffold, Biomolecules. 10 (2020) 684. https://doi.org/10.3390/biom10050684.

[9] C.A. Higgins, J.C. Chen, J.E. Cerise, C.A.B. Jahoda, A.M. Christiano, Microenvironmental reprogramming by threedimensional culture enables dermal papilla cells to induce de novo human hair-follicle growth, Proc. Natl. Acad. Sci. U. S. A. 110 (2013) 19679–19688. https://doi.org/10.1073/pnas.1309970110.

[10] V.A. Botchkarev, J. Kishimoto, Molecular control of epithelial-mesenchymal interactions during hair follicle cycling, in: J. Investig. Dermatology Symp. Proc., Elsevier Masson SAS, 2003: pp. 46–55. https://doi.org/10.1046/j.1523-1747.2003.12171.x.

[11] V.M. Weaver, O.W. Petersen, F. Wang, C.A. Larabell, P. Briand, C. Damsky, M.J. Bissell, Reversion of the malignant phenotype of human breast cells in three-dimensional culture and in vivo by integrin blocking antibodies., J. Cell Biol. 137 (1997) 231–245. https://doi.org/10.1083/jcb.137.1.231.

[12] K. Bhadriraju, C.S. Chen, Engineering cellular microenvironments to improve cell-based drug testing., Drug Discov. Today. 7 (2002) 612–620. https://doi.org/10.1016/s1359-6446(02)02273-0.

[13] H. Baharvand, S.M. Hashemi, S. Kazemi Ashtiani, A. Farrokhi, Differentiation of human embryonic stem cells into hepatocytes in 2D and 3D culture systems in vitro., Int. J. Dev. Biol. 50 (2006) 645–652. https://doi.org/10.1387/ijdb.052072hb.

[14] R. Edmondson, J.J. Broglie, A.F. Adcock, L. Yang, Three-dimensional cell culture systems and their applications in drug discovery and cell-based biosensors, Assay Drug Dev. Technol. 12 (2014) 207–218. https://doi.org/10.1089/adt.2014.573.

[15] P.D. Benya, J.D. Shaffer, Dedifferentiated chondrocytes reexpress the differentiated collagen phenotype when cultured in agarose gels., Cell. 30 (1982) 215–224. https://doi.org/10.1016/0092-8674(82)90027-7.

[16] C.M. Nelson, M.J. Bissell, Modeling dynamic reciprocity: engineering three-dimensional culture models of breast architecture, function, and neoplastic transformation., Semin. Cancer Biol. 15 (2005) 342–352. https://doi.org/10.1016/j.semcancer.2005.05.001.

[17] K. Shield, M.L. Ackland, N. Ahmed, G.E. Rice, Multicellular spheroids in ovarian cancer metastases: Biology and pathology., Gynecol. Oncol. 113 (2009) 143–148. https://doi.org/10.1016/j.ygyno.2008.11.032.

[18] M. Zietarska, C.M. Maugard, A. Filali-Mouhim, M. Alam-Fahmy, P.N. Tonin, D.M. Provencher, A.-M. Mes-Masson, Molecular description of a 3D in vitro model for the study of epithelial ovarian cancer (EOC)., Mol. Carcinog. 46 (2007) 872–885. https://doi.org/10.1002/mc.20315.

[19] B. Lin, Y. Miao, J. Wang, Z. Fan, L. Du, Y. Su, B. Liu, Z. Hu, M. Xing, Surface Tension Guided Hanging-Drop: Producing Controllable 3D Spheroid of High-Passaged Human Dermal Papilla Cells and Forming Inductive Microtissues for Hair-Follicle Regeneration., ACS Appl. Mater. Interfaces. 8 (2016) 5906–5916. https://doi.org/10.1021/acsami.6b00202.

[20] M. Ohyama, Y. Zheng, R. Paus, K.S. Stenn, The mesenchymal component of hair follicle neogenesis: background, methods and molecular characterization, Exp. Dermatol. 19 (2010) 89–99. https://doi.org/https://doi.org/10.1111/j.1600-0625.2009.00935.x.

[21] M. Bejaoui, M.O. Villareal, H. Isoda, 3,4,5-Tri-O-Caffeoylquinic Acid Promoted Hair Pigmentation Through β-Catenin and Its Target Genes, Front. Cell Dev. Biol. 8 (2020) 1–14. https://doi.org/10.3389/fcell.2020.00175.

[22] M. Bejaoui, M.O. Villareal, H. Isoda, β-catenin-mediated hair growth induction effect of 3,4,5-tri-O-caffeoylquinic acid, Aging (Albany. NY). 11 (2019) 4216–4237. https://doi.org/10.18632/aging.102048.

[23] M. Bejaoui, F. Ferdousi, Y.-W. Zheng, T. Oda, H. Isoda, Regulating cell fate of human amnion epithelial cells using natural compounds: an example of enhanced neural and pigment differentiation by 3,4,5-tri-O-caffeoylquinic acid, Cell Commun. Signal. 19 (2021) 26. https://doi.org/10.1186/s12964-020-00697-5.

[24] D.W. Huang, B.T. Sherman, R.A. Lempicki, Bioinformatics enrichment tools: Paths toward the comprehensive functional analysis of large gene lists, Nucleic Acids Res. 37 (2009) 1–13. https://doi.org/10.1093/nar/gkn923.

[25] D.W. Huang, B.T. Sherman, R.A. Lempicki, Systematic and integrative analysis of large gene lists using DAVID bioinformatics resources, Nat. Protoc. 4 (2009) 44–57. https://doi.org/10.1038/nprot.2008.211.

[26] A. Subramanian, P. Tamayo, V.K. Mootha, S. Mukherjee, B.L. Ebert, M.A. Gillette, A. Paulovich, S.L. Pomeroy, T.R. Golub, E.S. Lander, J.P. Mesirov, Gene set enrichment analysis: A knowledge-based approach for interpreting genome-wide expression profiles, Proc. Natl. Acad. Sci. U. S. A. 102 (2005) 15545–15550. https://doi.org/10.1073/pnas.0506580102.

[27] S. Hu, Z. Li, H. Lutz, K. Huang, T. Su, J. Cores, P.-U.C. Dinh, K. Cheng, Dermal exosomes containing miR-218-5p promote hair regeneration by regulating β-catenin signaling, Sci. Adv. 6 (2020) eaba1685. https://doi.org/10.1126/sciadv.aba1685.

[28] C.A.B. Jahoda, K.A. Horne, R.F. Oliver, Induction of hair growth by implantation of cultured dermal papilla cells, Nature. 311 (1984) 560–562. https://doi.org/10.1038/311560a0.

[29] C.A.B. Jahoda, R.F. Oliver, Vibrissa dermal papilla cell aggregative behaviour in vivo and in vitro, J. Embryol. Exp. Morphol. 79 (1984) 211 LP – 224. http://dev.biologists.org/content/79/1/211.abstract.

[30] R. Schmidt-Ullrich, R. Paus, Molecular principles of hair follicle induction and morphogenesis, BioEssays. 27 (2005) 247–261. https://doi.org/https://doi.org/10.1002/bies.20184.

[31] A. Osada, T. Iwabuchi, J. Kishimoto, T.S. Hamazaki, H. Okochi, Long-Term Culture of Mouse Vibrissal Dermal Papilla Cells and De Novo Hair Follicle Induction, Tissue Eng. 13 (2007) 975–982. https://doi.org/10.1089/ten.2006.0304.

[32] C.A.B. Jahoda, Cellular and developmental aspects of androgenetic alopecia, Exp. Dermatol. 7 (1998) 235–248. https://doi.org/https://doi.org/10.1111/j.1600-0625.2007.00666.x.

[33] A.G. MESSENGER, H. JENNIFER SENIOR, S.S. BLEEHEN, The in vitro properties of dermal papilla cell lines established from human hair follicles, Br. J. Dermatol. 114 (1986) 425–430. https://doi.org/https://doi.org/10.1111/j.1365-2133.1986.tb02846.x.

[34] T.-H. Young, H.-R. Tu, C.-C. Chan, Y.-C. Huang, M.-H. Yen, N.-C. Cheng, H.-C. Chiu, S.-J. Lin, The enhancement of dermal papilla cell aggregation by extracellular matrix proteins through effects on cell-substratum adhesivity and cell motility., Biomaterials. 30 (2009) 5031–5040. https://doi.org/10.1016/j.biomaterials.2009.05.065.

[35] Y. Miao, Y. Bin Sun, B.C. Liu, J.D. Jiang, Z.Q. Hu, Controllable production of transplantable adult human high-passage dermal papilla spheroids using 3D matrigel culture, Tissue Eng. Part A. 20 (2014) 2329–2338. https://doi.org/10.1089/ten.TEA.2013.0547.

[36] M. Rendl, L. Lewis, E. Fuchs, Molecular dissection of mesenchymal-epithelial interactions in the hair follicle., PLoS Biol. 3 (2005) e331. https://doi.org/10.1371/journal.pbio.0030331.

[37] A. Madaan, R. Verma, A.T. Singh, M. Jaggi, Review of Hair Follicle Dermal Papilla cells as in vitro screening model for hair growth, Int. J. Cosmet. Sci. 40 (2018) 429–450. https://doi.org/https://doi.org/10.1111/ics.12489.

[38] N.J. Combates, C.-M. Chuong, K.S. Stenn, S.M. Prouty, Expression of Two Ig Family Adhesion Molecules in the Murine Hair Cycle: DCC in the Bulge Epithelia and NCAM in the Follicular Papilla, J. Invest. Dermatol. 109 (1997) 672–678. https://doi.org/https://doi.org/10.1111/1523-1747.ep12337725.

[39] S.A. Ting-Berreth, C.-M. Chuong, Sonic hedgehog in feather morphogenesis: Induction of mesenchymal condensation and association with cell death, Dev. Dyn. 207 (1996) 157–170. https://doi.org/https://doi.org/10.1002/(SICI)1097-0177(199610)207:2<157::AID-AJA4>3.0.CO;2-G.

[40] D.L. du Cros, R.G. LeBaron, J.R. Couchman, Association of versican with dermal matrices and its potential role in hair follicle development and cycling., J. Invest. Dermatol. 105 (1995) 426–431. https://doi.org/10.1111/1523-1747.ep12321131.

[41] C.A. Higgins, G.D. Richardson, D. Ferdinando, G.E. Westgate, C.A.B. Jahoda, Modelling the hair follicle dermal papilla using spheroid cell cultures., Exp. Dermatol. 19 (2010) 546–548. https://doi.org/10.1111/j.1600-0625.2009.01007.x.

[42] K. Yamauchi, A. Kurosaka, Inhibition of glycogen synthase kinase-3 enhances the expression of alkaline phosphatase and insulin-like growth factor-1 in human primary dermal papilla cell culture and maintains mouse hair bulbs in organ culture, Arch. Dermatol. Res. 301 (2009) 357–365. https://doi.org/10.1007/s00403-009-0929-7.

[43] C.M. Abreu, M.T. Cerqueira, R.P. Pirraco, L. Gasperini, R.L. Reis, A.P. Marques, Rescuing key native traits in cultured dermal papilla cells for human hair regeneration, J. Adv. Res. 30 (2021) 103–112. https://doi.org/https://doi.org/10.1016/j.jare.2020.10.006.

[44] O. Mori, H. Uno, The effect of topical minoxidil on hair follicular cycles of rats., J. Dermatol. 17 (1990) 276–281. https://doi.org/10.1111/j.1346-8138.1990.tb01641.x.

[45] V.H. Price, E. Menefee, P.C. Strauss, Changes in hair weight and hair count in men with androgenetic alopecia, after application of 5% and 2% topical minoxidil, placebo, or no treatment., J. Am. Acad. Dermatol. 41 (1999) 717–721. https://doi.org/10.1016/s0190-9622(99)70006-x.

[46] P. Suchonwanit, S. Thammarucha, K. Leerunyakul, Minoxidil and its use in hair disorders: a review, Drug Des. Devel. Ther. 13 (2019) 2777–2786. https://doi.org/10.2147/DDDT.S214907.

[47] A.G. Messenger, J. Rundegren, Minoxidil: mechanisms of action on hair growth., Br. J. Dermatol. 150 (2004) 186–194. https://doi.org/10.1111/j.1365-2133.2004.05785.x.

[48] H. Shin, M.H. Kwack, S.H. Shin, J.W. Oh, B.M. Kang, A.A. Kim, J. Kim, M.K. Kim, J.C. Kim, Y.K. Sung, Identification of transcriptional targets of Wnt/beta-catenin signaling in dermal papilla cells of human scalp hair follicles: EP2 is a novel transcriptional target of Wnt3a., J. Dermatol. Sci. 58 (2010) 91–96. https://doi.org/10.1016/j.jdermsci.2010.02.011.

[49] R.L. Rajendran, P. Gangadaran, S.S. Bak, J.M. Oh, S. Kalimuthu, H.W. Lee, S.H. Baek, L. Zhu, Y.K. Sung, S.Y. Jeong, S.-W. Lee, J. Lee, B.-C. Ahn, Extracellular vesicles derived from MSCs activates dermal papilla cell in vitro and promotes hair follicle conversion from telogen to anagen in mice., Sci. Rep. 7 (2017) 15560. https://doi.org/10.1038/s41598-017-15505-3.

[50] K. Adachi, Y. Watanabe, K. Inouye, Activity of glucose-6-phosphate 1-dehydrogenase in hair follicles with male-pattern alopecia, Biosci. Biotechnol. Biochem. 63 (1999). https://doi.org/10.1271/bbb.63.2219.

[51] M. Ohyama, T. Kobayashi, T. Sasaki, A. Shimizu, M. Amagai, Restoration of the intrinsic properties of human dermal papilla in vitro, J. Cell Sci. 125 (2012) 4114–4125. https://doi.org/10.1242/jcs.105700.

[52] V. Horsley, A.O. Aliprantis, L. Polak, L.H. Glimcher, E. Fuchs, NFATc1 Balances Quiescence and Proliferation of Skin Stem Cells, Cell. 132 (2008) 299–310. https://doi.org/10.1016/j.cell.2007.11.047.

[53] B.E. Keyes, J.P. Segal, E. Heller, W.-H. Lien, C.-Y. Chang, X. Guo, D.S. Oristian, D. Zheng, E. Fuchs, Nfatc1 orchestrates aging in hair follicle stem cells, Proc. Natl. Acad. Sci. 110 (2013) E4950–E4959. https://doi.org/10.1073/pnas.1320301110.

[54] E. Avigad Laron, E. Aamar, D. Enshell-Seijffers, The Mesenchymal Niche of the Hair Follicle Induces Regeneration by Releasing Primed Progenitors from Inhibitory Effects of Quiescent Stem Cells, Cell Rep. 24 (2018) 909-921.e3. https://doi.org/10.1016/j.celrep.2018.06.084.

[55] T. Soma, M. Tajima, J. Kishimoto, Hair cycle-specific expression of versican in human hair follicles., J. Dermatol. Sci. 39 (2005) 147–154. https://doi.org/10.1016/j.jdermsci.2005.03.010.

[56] S.R. Kim, S.Y. Cha, M.K. Kim, J.C. Kim, Y.K. Sung, Induction of versican by ascorbic acid 2-phosphate in dermal papilla cells., J. Dermatol. Sci. 43 (2006) 60–62. https://doi.org/10.1016/j.jdermsci.2006.02.010.

[57] Y. Takabayashi, M. Nambu, M. Ishihara, M. Kuwabara, K. Fukuda, S. Nakamura, H. Hattori, T. Kiyosawa, Enhanced effect of fibroblast growth factor-2-containing dalteparin/protamine nanoparticles on hair growth, Clin. Cosmet. Investig. Dermatol. 9 (2016) 127–134. https://doi.org/10.2147/CCID.S108187.

[58] W. Lin, L.-J. Xiang, H.-X. Shi, J. Zhang, L. Jiang, P. Cai, Z.-L. Lin, B.-B. Lin, Y. Huang, H.-L. Zhang, X.-B. Fu, D.-J. Guo, X.-K. Li, X.-J. Wang, J. Xiao, Fibroblast Growth Factors Stimulate Hair Growth throughβ-Catenin and Shh Expression in C57BL/6 Mice, Biomed Res. Int. 2015 (2015) 1–9. https://doi.org/10.1155/2015/730139.

[59] S. Maretto, M. Cordenonsi, S. Dupont, P. Braghetta, V. Broccoli, A.B. Hassan, D. Volpin, G.M. Bressan, S. Piccolo, Mapping Wnt/ -catenin signaling during mouse development and in colorectal tumors, Proc. Natl. Acad. Sci. 100 (2003) 3299–3304. https://doi.org/10.1073/pnas.0434590100.

[60] T. Andl, S.T. Reddy, T. Gaddapara, S.E. Millar, WNT signals are required for the initiation of hair follicle development, Dev. Cell. 2 (2002) 643–653. https://doi.org/10.1016/S1534-5807(02)00167-3.

[61] B.Y. Choi, Targeting Wnt/β-Catenin Pathway for Developing Therapies for Hair Loss, Int. J. Mol. Sci. 21 (2020) 4915. https://doi.org/10.3390/ijms21144915.

[62] K. Katsuoka, C. Mauch, H. Schell, O.P. Hornstein, T. Krieg, Collagen-type synthesis in human-hair papilla cells in culture, Arch. Dermatol. Res. 280 (1988) 140–144. https://doi.org/10.1007/BF00456843.

Tables

Table 1: List of DEGs in 3D spheroid compared with 2D culture *

Gene symbol	Gene name	Biological function	Fold-change	*P* value **
OXTR	Oxytocin receptor	Cell surface receptor signalling pathway; oxidative stress	24.82	0.0002
COL11A1	Collagen alpha-1 (XI) chain	Extracellular matrix binding	21.67	0.003
SSTR1	Somatostatin receptor type 1	Expressed during anagen phase; HF immune system	21.03	0.001
NEDD9	Enhancer of filamentation 1	Cell adhesion; hair placode signature genes	18.48	0.004
HAPLN1	Hyaluronan and proteoglycan link protein 1	Cell adhesion; cell-cell communication	14.06	0.005
IL8	Interleukin-8	Immune response; inflammation	-179.99	0.004
TNFAIP6	Tumor necrosis factor-inducible gene 6 protein	TNF-α signalling; inflammation	-32	0.001
RANBP3L	Ran-binding protein 3-like	Termination of BMP signalling; inhibition of mesenchymal stem cell differentiation	-31.18	0.003
GDF15	Growth/differentiation factor 15	Stress response cytokine, expression increases with inflammation and injury	-25.96	0.045

*Table 2: Top upregulated genes in 3D minoxidil-treated cells (vs 3D control) *.*

Gene symbol	Gene name	Biological function	Fold-change	*P* value **
CTNNB1	Catenin (cadherin associated protein), beta 1	Anagen phase regulation; hair follicle morphogenesis; positive regulation of fibroblast growth, dermal papilla cells proliferation	19.06	0.049
TRH	Pro-thyrotropin-releasing hormone	Hair shaft elongation; anagen phase prolongation; hair matrix keratinocytes proliferation	7.25	0.011
RASGRF1	Ras-specific guanine nucleotide-releasing factor	Hair follicle morphogenesis; ATP binding	6.75	0.020
FERMT1	Fermitin family homolog 1	Cell adhesion; keratinocyte proliferation and morphogenesis	6.03	0.018
ABCC11	ATP-binding cassette sub-family C member 11	ATP binding	5.88	0.029
CXXC5	CXXC-type zinc finger protein 5	Involved in MAPK pathway; cell cycle arrest	5.11	0.021
NCAM	Neural cell adhesion molecule	Hair morphogenesis; highly expressed during anagen phase; keratinocytes segregation and differentiation	4.72	0.085
COL28A1	Collagen alpha-1(XXVIII) chain	Hair shaft strength; matrix assembly	4.62	0.006
KRT40	Keratin, type I cytoskeletal 40	Late hair differentiation	4.06	0.010
VCAN	Versican	Collagen-containing extracellular matrix; highly expressed during anagen phase	3.23	0.008

Table 3: Top downregulated genes in 3D minoxidil-treated cells (vs 3D control).*

Gene symbol	Gene name	Biological function	Fold-change	*P* value **
NFATC1	Nuclear factor of activated T cells, cytoplasmic, calcineurin dependent 1	Stem cells quiescence	-8.22	0.001
STEAP3	STEAP family member 3	Inhibition of cell cycle arrest, downregulation of P53 pathway	-7.96	0.003
LFNG	LFNG O-fucosylpeptide 3-beta-N-acetylglucosaminyltransferase	Notch pathway inhibition; decrease hair development	-7.07	0.011
PRUNE2	Protein prune homolog 2	Regulation of tumor cells differentiation, survival and aggressiveness	-6.82	0.032
SKIV21	Superkiller viralicidic activity 2-lik	ATP degradation	-5.45	0.007
TRABD2B	TraB domain containing 2B	Negative regulator of the Wnt pathway; Wnt protein cleavage	-5.04	0.027
MAF	Avian musculoaponeurotic fibrosarcoma oncogene homolog	Oncogene; embryonic marker of development	-4.78	0.062
STYK1	Serine/threonine/tyrosine kinase 1	Tumor cell invasion and metastasis	-3.42	0.012
AXIN2	Axin 2	β-Catenin phosphorylation and degradation	-3.33	0.028
SIX3	Sine oculis-related homeobox 3	Wnt/β-Catenin repression	-2.74	0.005

Table 4: Comparison between TCQA-treated HFDPCs in 2D, 3D, and in vivo [22]*.

Gene symbol	Gene name	Biological function	Fold-change		
			2D	3D	*in vivo*
CTNNB1	Catenin (cadherin associated protein), beta 1	Anagen phase regulation; hair follicle morphogenesis; positive regulation of fibroblast growth, dermal papilla cells proliferation	1.62	43.57	3.2
FGF1	Fibroblast growth factor 1	Hair follicle morphogenesis; hair growth cycle regulation	1.53	26.45	3.22
NRAS	Neuroblastoma RAS viral oncogene homolog	Cell proliferation	1.53	16	1.2
ALPL	Alkaline phosphatase	Wnt/β-catenin pathway regulator	1.2	8	2.33
BMPR-1A	Bone morphogenetic protein	Skin development; hair follicle growth	1.14	64.89	1.7
VCAN	Versican	Cell aggregation marker; Cell adhesion and proliferation	4.61	12.21	1.6
WLS	Wntless	Wnt secretion and pathway	1.6	16.38	3
AXIN2	Axis inhibition protein 2	Wnt-responsive gene	-1.5	-5	-2.82
TCF3	Transcription factor 3	Wnt/β-Catenin repression	-1.1	-5	-2.82
LDB3	LIM Domain Binding 3	Wnt-responsive gene; Regulation of hair follicle during telogen	-1.14	-2.7	-8.7
EGR1	Early growth response 1	Negative regulation of Wnt/β-Catenin; upregulated with aging	-1.7	-4	-2.6
GSK3B	Glycogen synthase kinase 3 beta	Phosphorylation of β-catenin	-1.5	-6	-5

For all Tables

*Genes functions were obtained from Mouse Genome Informatics (MGI).

**ANOVA was performed to assess the level of significance between groups. The gene expression was considered significant when fold change was ≥ 2-fold (control vs TCQA

Figures

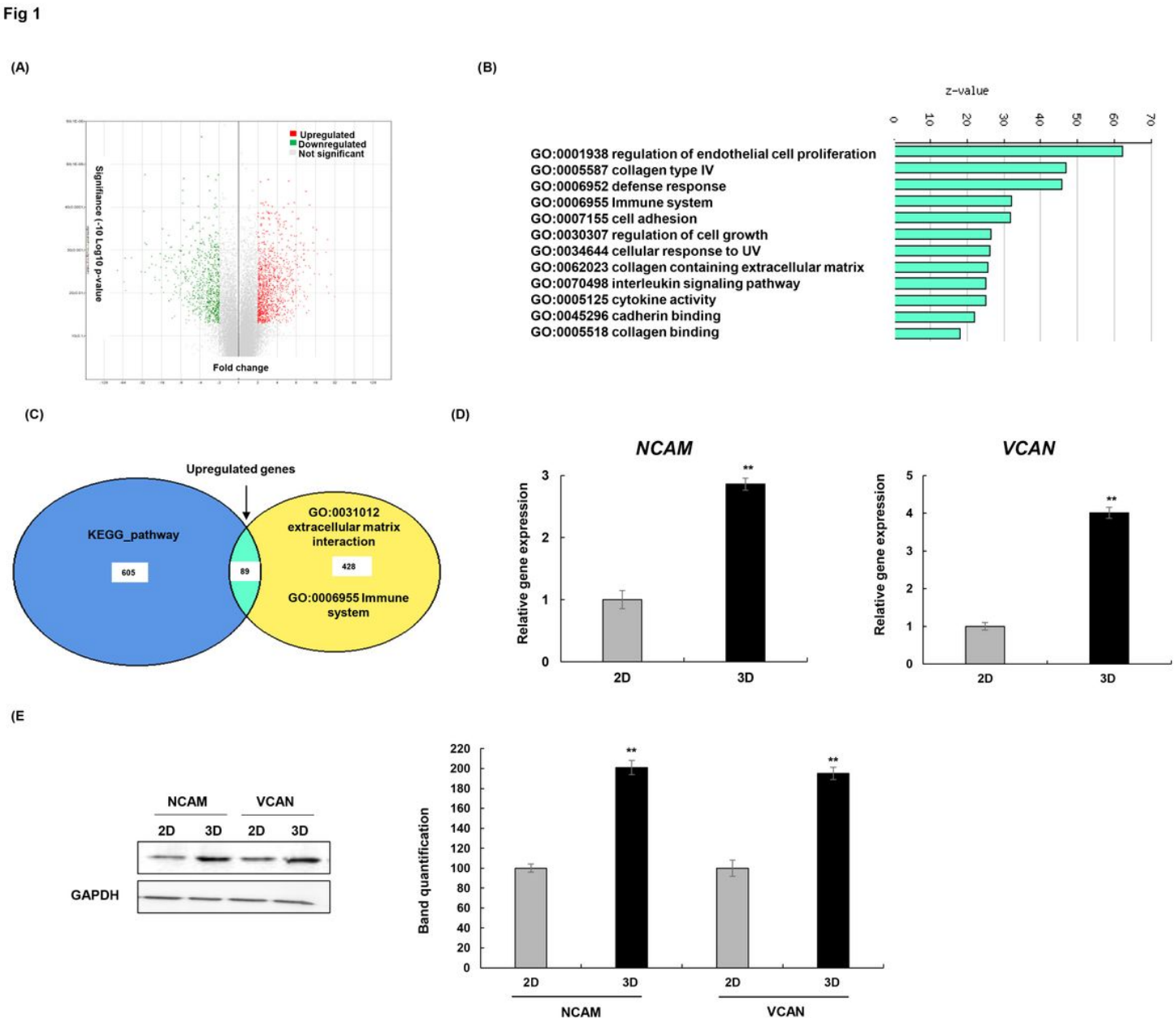

Figure 1

Gene profiling analysis of HFDPC cultured in 3D spheroid vs 2D monolayer. (A) Volcano plot showing the DEGs. The colors: red, green, and grey illustrated the upregulated, downregulated, and nonsignificant

DEGs, respectively. (B) Top 12 significantly enriched biological processes by the upregulated DEGs (analyzed using Ex atlas). (C) Venn diagram showing common and unique sets of DEGs. (D) Gene expression of VCAN and NCAM after 48 h. The mRNA level was quantified using TaqMan real-time PCR (E) VCAN and NCAM protein expression after 48 h. Band intensities was assessed using LICOR system. Results represent the mean ± SD of three independent experiments. * P ≤0.05, ** P ≤0.01.

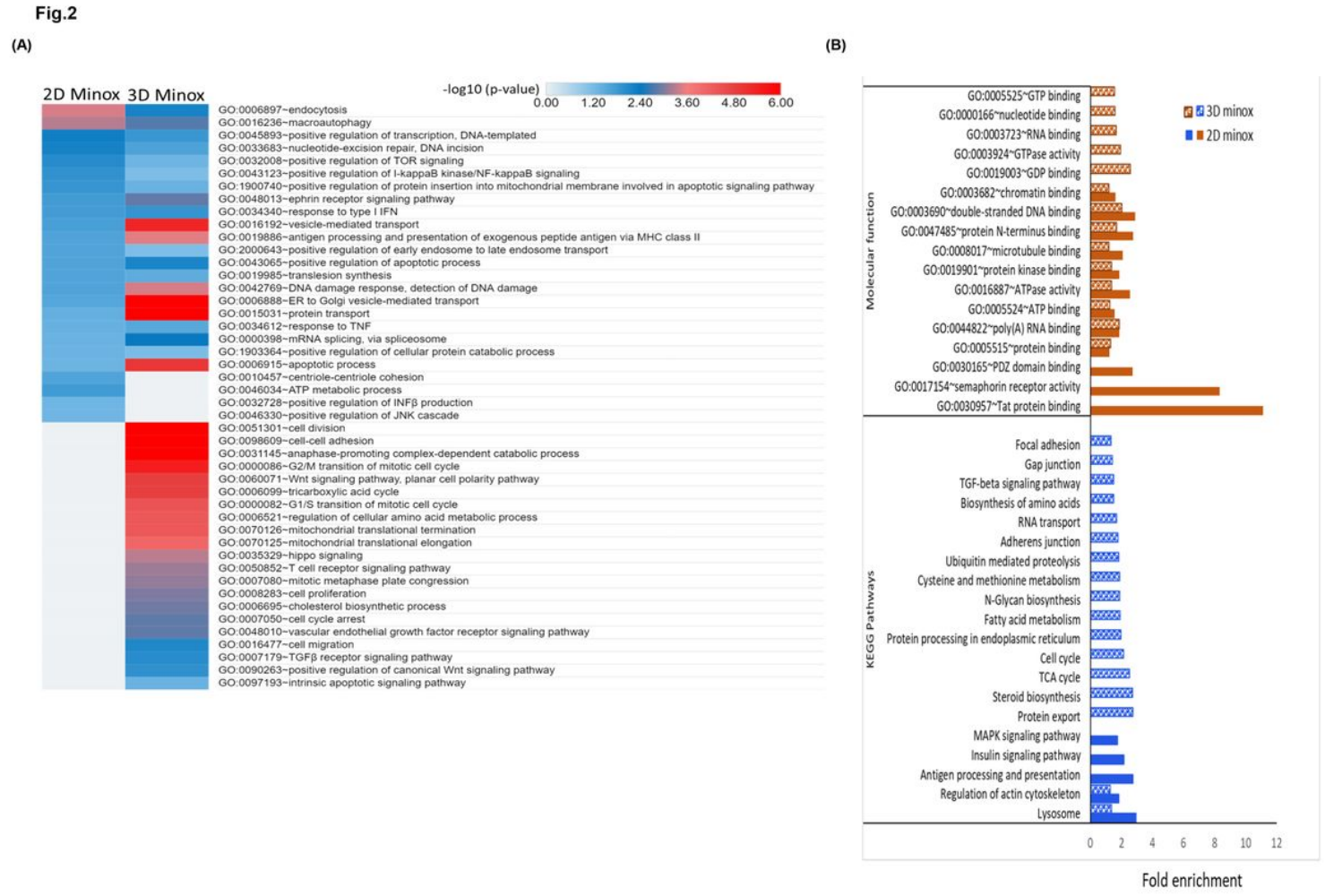

Figure 2

Microarray analysis comparing 2D minoxidil vs 2D control and 3D minoxidil vs 3D control. (A) Scatter plot Scatter plot showing the DEGs for 2D minoxidil vs 2D control (left) and 3D minoxidil vs 3D control (right). (B) Scatter plot showing the DEGs for 3D minoxidil vs 3D control.The yellow color represents the upregulated DEGs, green color represents the downregulated DEGs, and grey color represents the nonsignificant genes. (C) Classification of DEGs according to fold change in compared sets. (D) Heat

map showing the significance of biological processes in 4 comparison sets. Heat map was generated using Morpheus online software (https://software.broadinstitute.org/morpheus).

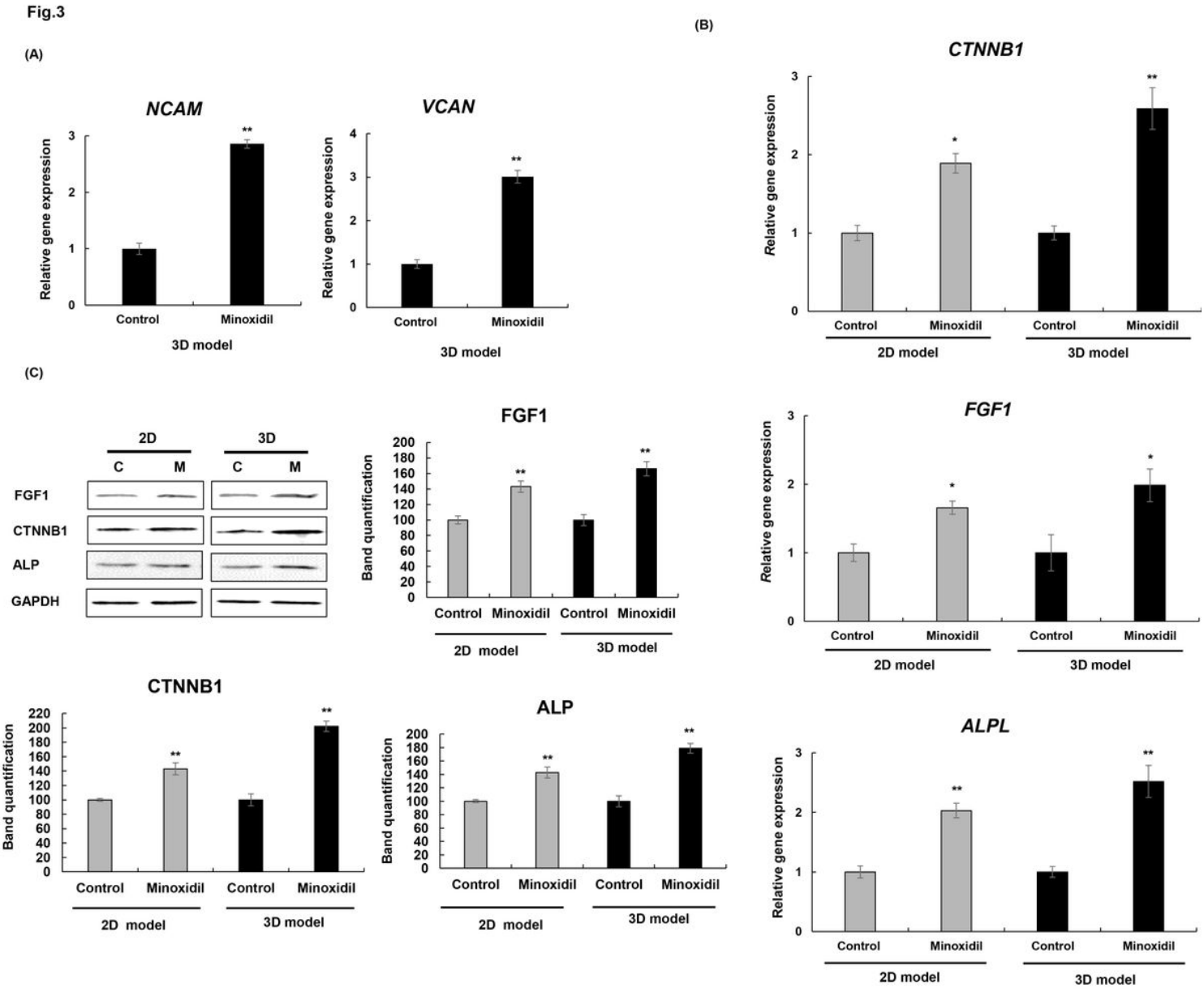

Figure 3

Comparison of GO between 3D minoxidil vs 2D minoxidil. (A) Top significantly enriched biological processes by regulated DEGs. (B) Top significantly enriched molecular process and KEGG pathway by regulated DEGs (analysed using DAVID and GSEA).

Fig.4

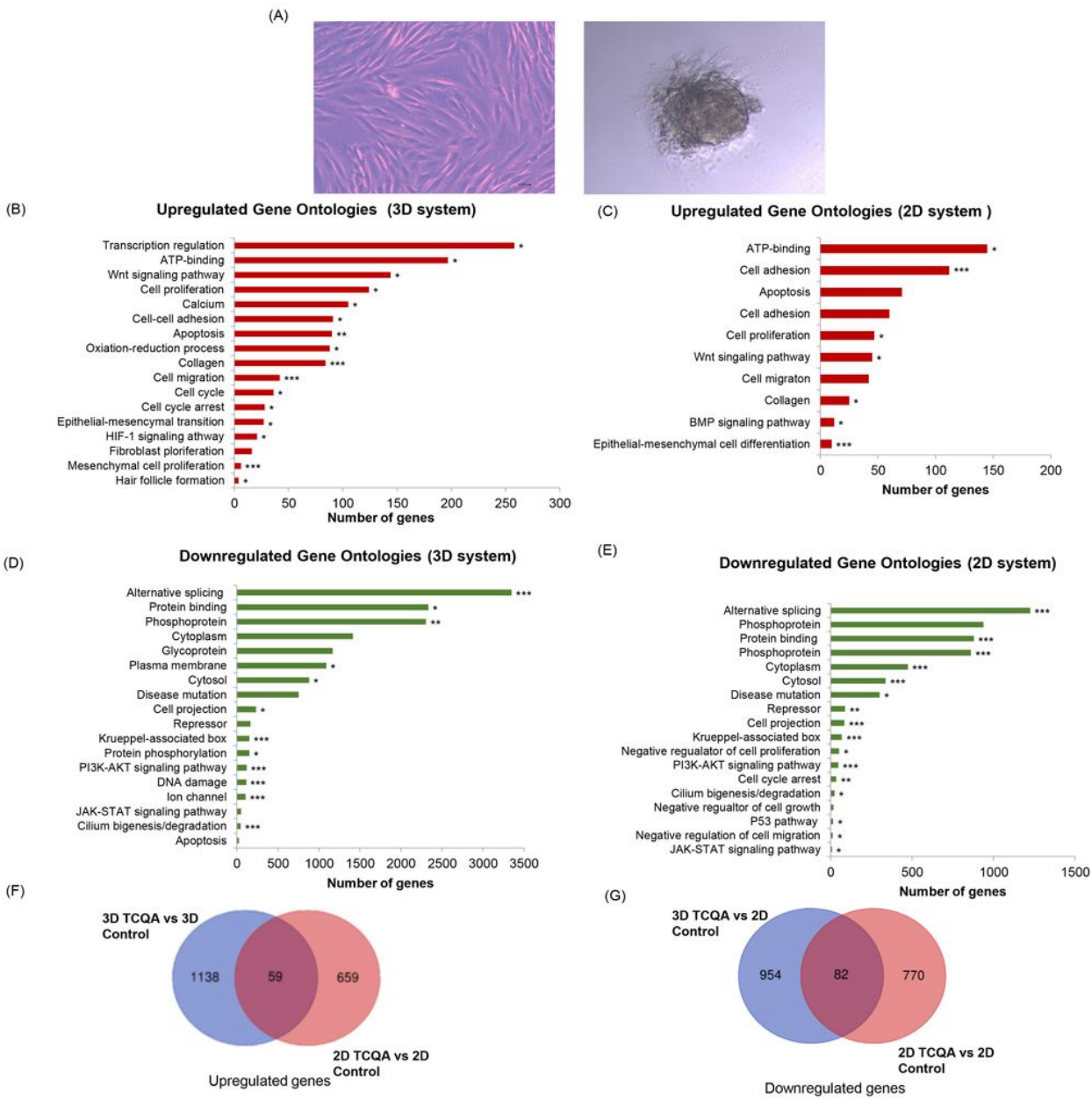

Figure 4

Expression of ECM and hair growth markers upon minoxidil treatment in 3D and 2D systems. (A) Gene expression of ECM markers: VCAN and NCAM after 48 h. (B) Gene expression of hair growth markers: CTNNB1, ALPL, and FGF1 after 48 h. For A and B, The mRNA level was quantified using TaqMan real-time PCR. Results represent the mean ± SD of three independent experiments. (C) β-catenin, ALP, and FGF1 protein expression after 48 h. Band intensities was assessed using LICOR system. Results represent the mean ± SD of three independent experiments. * P ≤0.05, ** P ≤0.01.

Fig.5

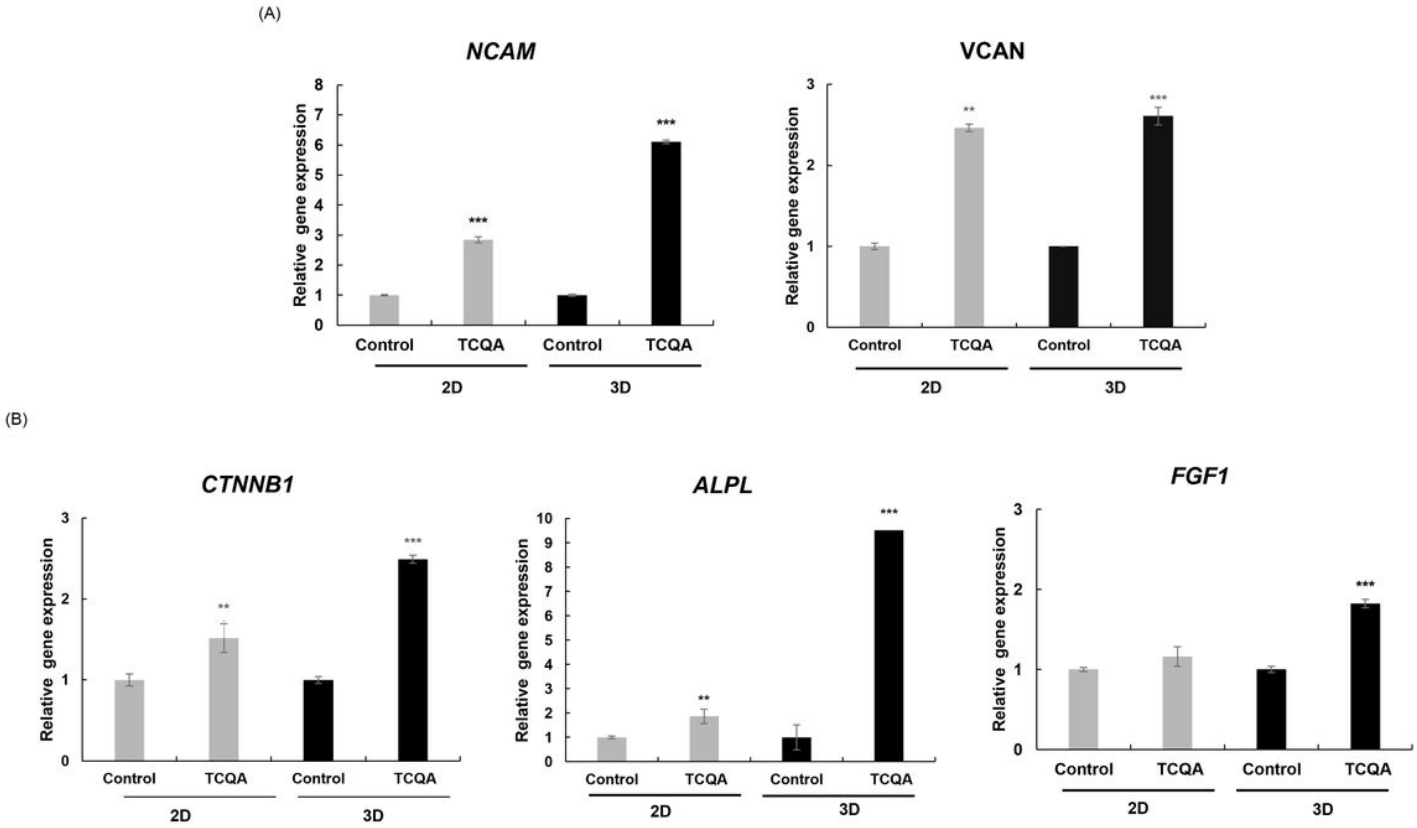

Figure 5

Efficacy comparison of 2D and 3D systems on HDFPC treated with TCQA. (A) Morphological difference of 2D (left) and 3D (right) cultured HFDPC treated with TCQA. (B) Top significantly enriched biological processes in 3D system treated with TCQA. (C) Top significantly enriched biological processes in 2D system treated with TCQA. (D) Top significantly downregulated biological processes in 3D system treated with TCQA. (E) Top significantly downregulated biological processes in 2D system treated with TCQA (Gene sets, are analysed using DAVID). The Student's t-test was used and * $P \leq 0.05$, ** $P \leq 0.01$.Venn diagrams showing the overlapping and unique (F) upregulated and (G) downregulated DEGs of 2D (TCQA) vs Control and 3D (TCQA) vs Control.

Figure 6

Expression of ECM and hair growth markers upon treatment of TCQA in 3D and 2D systems. (A) Gene expression of ECM markers: VCAN and NCAM after 48 h. (B) Gene expression of hair growth markers: CTNNB1, ALPL, and FGF1 after 48 h. The mRNA level was quantified using TaqMan real-time PCR. Results represent the mean ± SD of three independent experiments. The Student's t-test was used to compare the mean values of two groups, * P ≤0.05, ** P ≤0.01, *** P ≤0.001.

Supplementary Files

This is a list of supplementary files associated with this preprint. Click to download.

- SuppFigures.pdf
- SuppTables.docx